Electronic structure of metal phthalocyanines on Ag (100)

Cornelius Krull

Ph.D. Thesis

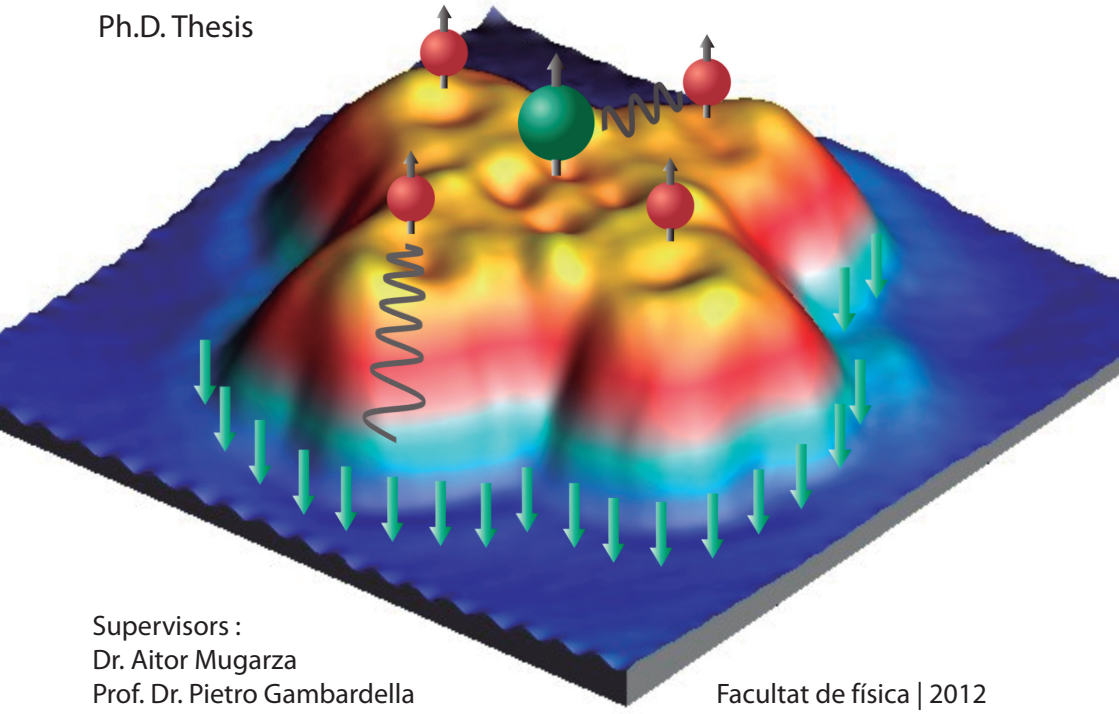

Supervisors :
Dr. Aitor Mugarza
Prof. Dr. Pietro Gambardella

Facultat de física | 2012

Institut Català de Nanotecnologia
Universitat Autònoma de Barcelona

Chapter 6

6 Doping of MePc: Alkali and Fe atoms

In this chapter we will explore the possibility to manipulate the charge and spin states of MePcs by adding dopant adatoms. To dope the molecules with additional electrons, we codeposited them with a known electron donor alkali atoms, Lithium (Li). In a second experiment, we studied the interaction of NiPc and CuPc, with magnetic Fe adatoms, as a more direct way to influence the molecular magnetic moment.

6.1. Electron doping of MePc

In "traditional" electronics a common approach to achieve a desired electronic structure is the doping of semiconductors. This idea has been carried over to molecular electronics. Consequently considerable research has been done on electron/hole doping of thin organic films: in purely organic films of simple molecules such as C_{60}, the large extension of the π orbitals results in a reduced Coulomb repulsion. Here the scenario is rather simple, electron doping leads to a rigid, continuous, multiple filling of the LUMO [219, 220, 221].

On the other hand MePcs, with localized d states coexisting with π orbitals near E_F, reveal a more complex behavior. Previous experiments on MePc thin films (50-100 nm) conclude that the doping depends mainly on the type of metal ion. Studies on Potassium (K) doped thin films of CoPc and FePc show the charging of the states derived from the Ion's d orbitals

[222, 223, 224]. In contrast, for NiPc and CuPc molecules the charging of the ligand LUMO is reported [222, 223, 225]. DFT calculations suggest that this behavior is due to the presence or absence of unfilled/partially filled d states close to E_F, as well as the metal ion´s on-site coulomb repulsion [177]. Furthermore in these thin films the crystal structure is deeply intertwined with the charging behavior. In K doped MePc crystals (Me= Fe [226], Cu [227], Zn [228]) a phase separation between K_2MePc and K_4MePc occurs. Each different structure allows a transfer of respectively 2 or 4 electrons to the molecule. A recent study of a CuPc monolayer on Au(110) shows the charging can go even further and involve not only the LUMO, but the LUMO+1 and LUMO+2, thus accepting more charge per CuPc [229]. The type of dopant used has an effect as well, Sodium and Rubidium doped CuPc films report the charging of the Cu ion without any phase separation [230, 231].

Nevertheless, the doping of single molecules at a metallic interface has not been studied so far, although it lies very well within the capabilities of an STM setup, as shown by the controlled doping of C_{60} with potassium [221]. The results presented in the previous chapters show that, already for undoped MePc molecules, a range of intriguing electronic and magnetic states can be achieved by different central metal ions. The atom-by-atom doping with Lithium atoms is the next step to further extend and tune the MePc's rich magnetic behavior.

In this section, the results of a comparative study of the Lithium doping of individual MePcs (Me= Fe, Co, Ni, Cu) using low temperature STM and DFT are presented. We will show that the charging behavior of these molecules adsorbed on an Ag(100) surface depends on the type of the central metal ion as well as the specific bonding configuration of the Li and molecule, allowing the specific charging of the ion or ligand states. In this fashion the total spin of individual CuPc molecules can be controlled from 0 to ½ and 1, as well as the additional charge from 1 to 2.

6.1.1. Single MePc doped with Lithium

Topography of Li@CuPc and Li@NiPc

The interaction between CuPc with Li atoms leads to several stable configurations, the two most frequent are presented in Figure 6.1a), denoted as L, M.

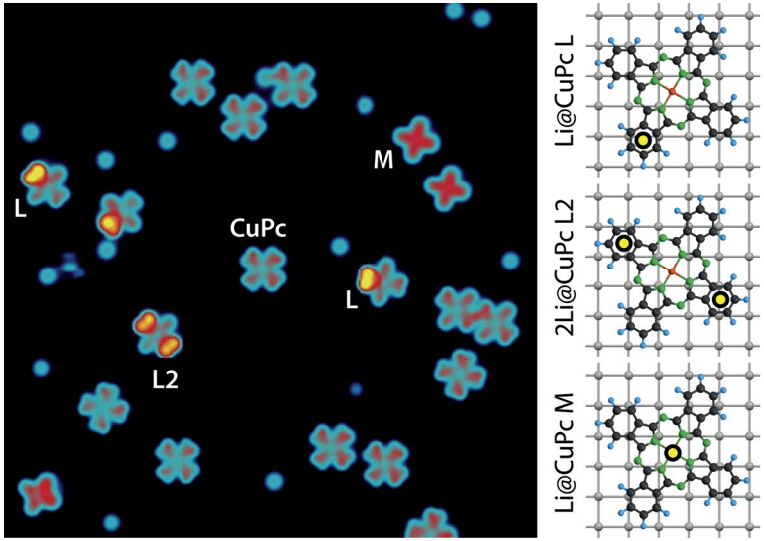

Figure 6.1.: a) STM topography image (-0.3 V, 0.17 nA, 19.3 nm x19.3 nm) of CuPc and Li atoms on Ag(100). Different types of xLi@CuPc complexes are marked with L and M, their proposed geometrical configurationa are shown on the right panels.

The type L(ligand) configuration exhibits two very bright protrusions on one of the benzene rings. From STM manipulation of Li atoms (see the discussion of Figure 6.10 on page 136) it becomes clear that this is the effect of one Li atom interacting with one of the benzene rings of the CuPc (see Figure 6.1). When two Li atoms interact with a CuPc, the bright protrusions are seen on two opposing benzene rings, the L2 type. Other configurations, such as Li adatoms in two neighboring benzene rings were not observed.

The location of Li seems to be under the benzene ring, as suggested by the missing signature of the Li atom, i.e., one circular protrusion, in both topographic images and spectroscopic maps. This theory is further supported by DFT calculations, as will be discussed later.

The type M(metal) configuration leads to a Li@CuPc with four-fold symmetric ligands, and a brighter center than an undoped CuPc, suggesting that one Li atom is located at the center of the molecule (see Figure 6.1). The rotational stability is affected by the Li, and some of the type M molecules are rotated (+14°; -42° with respect to the [011]

direction), whereas for the type L complexes no deviation from the $\pm 30^{o}$ orientation of the undoped CuPc were observed.

For Li@NiPc only the type L configuration is stable. A configuration that could be assigned to type M appears to be unstable, with a fuzzy ion site both in topography and spectroscopy (data not shown). The lower stability of this configuration in NiPc is also supported by the DFT calculations, as will be treated later on.

Electronic structure of Li@CuPc and Li@NiPc - orbital selectivity

To characterize the influence of the Li on the electronic structure, STS measurements were performed on two representative points of the molecule: on the center metal ion and on the benzene ring. Figure 6.2 shows the dI/dV spectra for Li@CuPc type L and M taken on the benzene rings.

In gas phase MePc molecules the empty $2e_g$ orbital is 2-fold degenerate, not considering the spin degree of freedom. For the CuPc/Ag(100) we found it be singly occupied, observing a peak below E_F, and an additional peak above E_F corresponding to the double occupation ($2e_g$+U) (see chapter 5). For both Li@CuPc types the $2e_g$ orbital is in a different configuration. In type M complexes a unoccupied single state is encountered. Its spatial distribution follows that of the $2e_g$, indicating that it is shifted above E_F, and no electrons neither from the substrate nor the Li are transferred to it. In type L complexes a double peak structure is recovered. In this case the degeneracy of the $2e_g$ state is lifted, and the MO is split into two separate states, denoted by greek letters α_{2eg} (occupied state) and β_{2eg} (unoccupied state). The reason for this is the symmetry reduction from C4v to C2v caused by the presence of Li, similar to the effect of a neighboring molecule discussed on page 104. This can be deduced from the two-fold symmetric, orthogonal molecular resonances mapped at each energy (see Figure 6.2), as opposed to the four-fold symmetric orbital mapped for both undoped and type M complexes ($2e_g$).

The occupied region shows a multi-peak structure, which we assign to the coupling of the α_{2eg} to vibrational modes of the molecule (see Figure 6.3).The energy found for these vibronic progressions is comparable to those observed in CuPc multilayers, as discussed in section 5.5.1 (pg. 116). Their existence is signature of a decoupling from the conduction electrons of the substrate.

In both cases the Kondo resonance is quenched, due to the changes

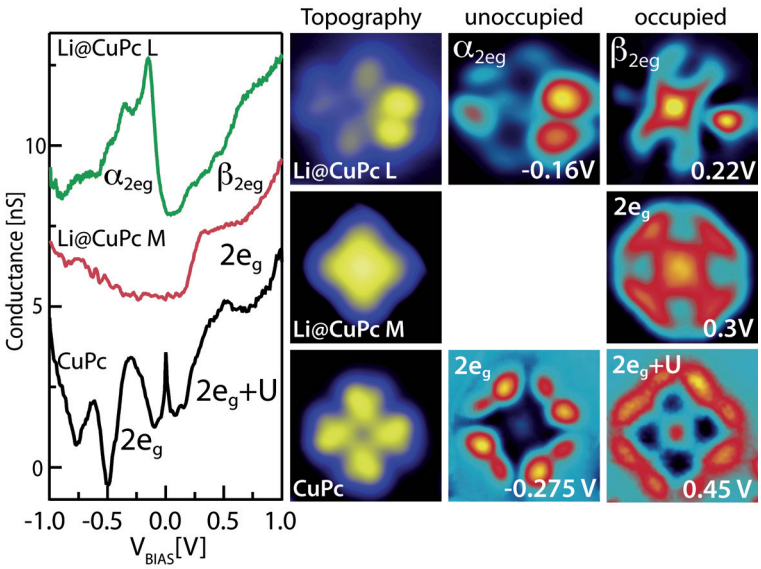

Figure 6.2.: dI/dV spectroscopy taken on one benzene ring of different xLi@CuPc complexes (-1 V, 1 nA) and CuPc (-2 V, 3 nA). Right panels: dI/dV maps 3 nm x3 nm, showing the intensity distribution of the marked features in the spectra. Note that for the L type the α_{2eg} and β_{2eg} states are orthogonal to each other.

in the $2e_g$ state. For type M this is readily explained from STS by the loss of the unpaired electron in the $2e_g$ orbital. The situation for type L is the opposite. The fact that we do not observe a double occupation peak above E_F, but rather the degeneracy split β_{2eg} state, suggests that the α_{2eg} orbital is completely filled. This interpretation is confirmed by DFT, showing a doubly occupied MO with one electron donated from Ag substrate and another from Li (see Table 6.1).

In the case of Li@NiPc only the type L complexes are stable. Although the topographic appearance is identical to Li@CuPc type L, there are several differences in the spectra. Figure 6.4 displays the dI/dV spectrum of the type L Li@NiPc, a sharply defined double peak structure above and below E_F is visible. The corresponding dI/dV maps show that the spatial distribution has a node at the axis intersecting the benzene with Li, indicating that they correspond to the same orbital (α_{2eg}). Additionally

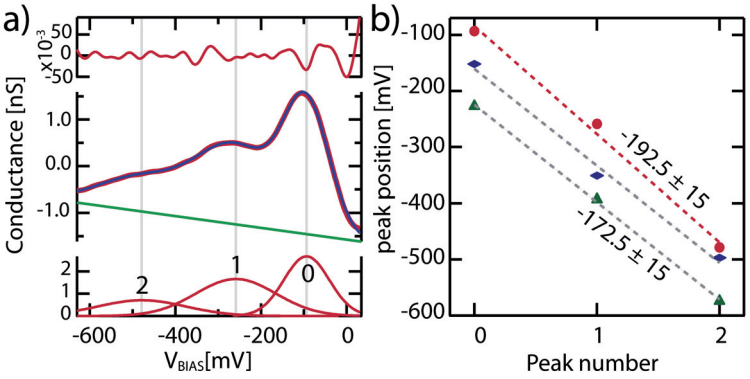

Figure 6.3.: a) Fit of the multi peak structure below E_F for Li@NiPc. The above curve shows the error of the fit, below the fitting peaks are presented. b) Peak position obtained from similar fits for different Li@MePc configurations. An equidistant peak spacing is visible, pointing to a vibronic origin of the multi-peak structure.

we expect the $2e_g$ state to be split due the presence of Li, as seen for Li@CuPc. In fact the orthogonal β_{2eg} state is found at slightly higher energy, meaning a completely empty orbital (see Figure 6.4). Based on the presence of a peak with α_{2eg} symmetry above E_F, we conclude that this state is singly occupied.

These observations imply that Li@NiPc L has only one added electron, as opposed to the two found for Li@CuPc L. This is confirmed by adding a second Li atom to the Li@NiPc L complex. The STS of 2Li@NiPc L becomes identical to that of Li@CuPc L. In this case the spatial distribution of the states found above and below E_F is clearly orthogonal (see Figure 6.4b), indicating a filled α_{2eg} and an unoccupied β_{2eg} state, an identical configuration to that of Li@CuPc L.

These results suggest that, adding the first Li to NiPc does not increase the total molecular charge, compared to the NiPc adsorbed on Ag(100). The addition of the second Li then adds an extra electron to the α_{2eg} state, thereby reaching the same charge configurations, as the singly doped Li@CuPc L complex.

These results show the impact of the central ion on the charging behavior even in the case of two very similar cases. MePcs with similar molecule substrate interaction like CuPc and NiPc can still present a different behavior upon charging. Instead of only donating charge to the

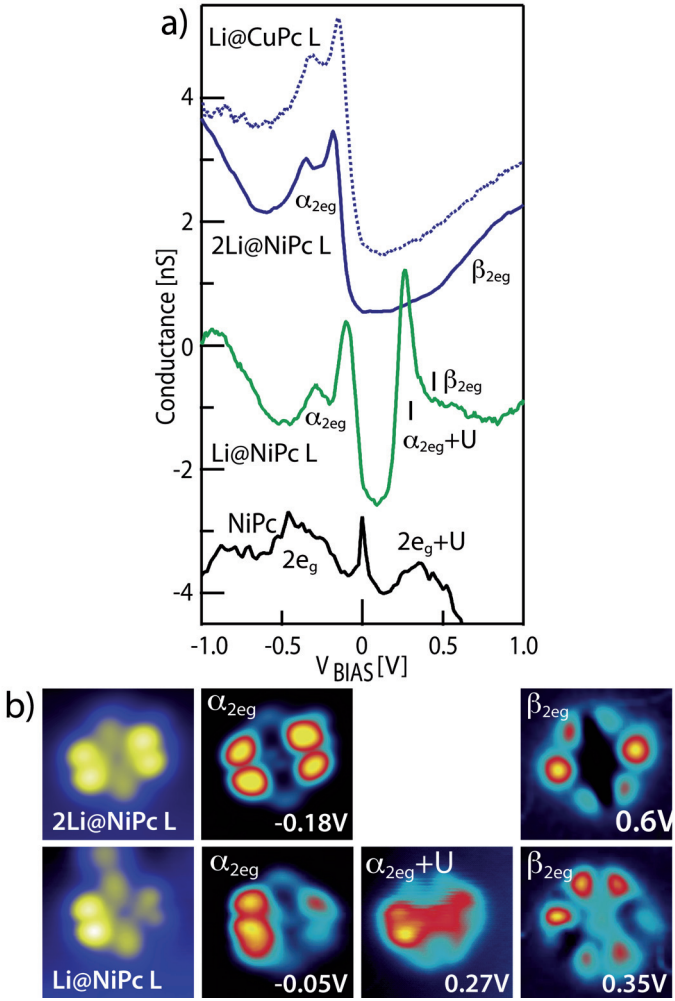

Figure 6.4.: a) dI/dV spectroscopy taken on one of the benzene rings of different the xLi@NiPc (-1 V, 1 nA). b) STM topography images and dI/dV maps 3 nm x3 nm, showing the charged and uncharged MO.

NiPc, the Li changes the way the molecule interacts with the substrate, decoupling it seen by the sharper resonances and the presence of vibronic coupling, and reducing the charge transfer from the substrate, as we will further discuss in the next section.

DFT:MePc with Li atoms

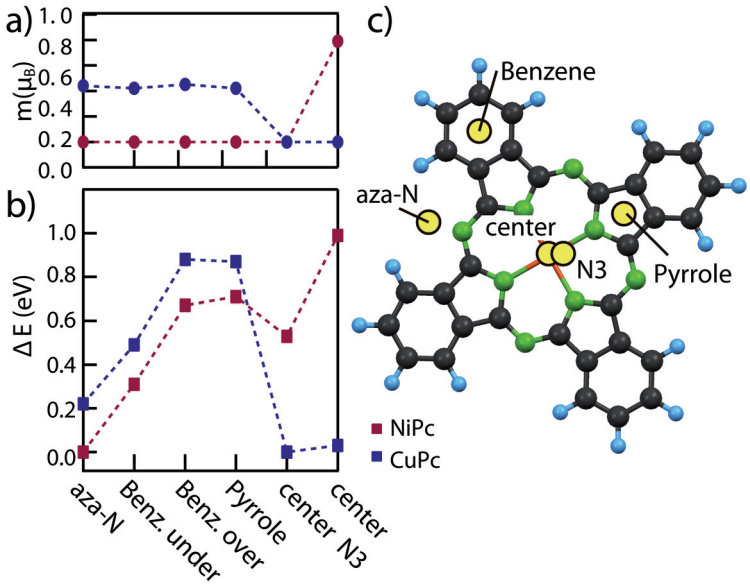

Figure 6.5.: DFT calculations for various positions of the Li adatom: a) Magnetic moment of the TM ion in μ_B, and b) relative formation energies for c) various positions of the Li. Note that for the center N3 configuration the charge is transferred to the $2e_g$ for NiPc whereas for CuPc to the b_{1g} orbital.

STS was able to detect the charging trend of the ligand π orbital for the different Li@MePc configurations, however the behavior of TM d states cannot be accessed as readily. Hence, the full electronic and magnetic structure of the charged molecules can only be understood with the aid of DFT calculations.

Six different configurations, depicted in 130c), have been explored by DFT. In four of them the Li ion interacts with the organic ligand, and in the other two with the metal ion. The relative energies plotted in Figure 6.5b), show a clear switch in the stability of configurations with Li interacting with the ion: for CuPc they are stable configurations, whereas for NiPc they are unstable. This explains the fuzzy images obtained for Li@NiPc with the Li at the center.

The configurations that involve a Li-ligand interaction, show trends

similar for both molecules: the most stable one places the Li outside the molecule close to the aza-N, and the second most stable has the Li under a benzene ring. All four configurations, considering the Li-ligand bond, show the same electronic structure, regardless of the exact position of the Li.

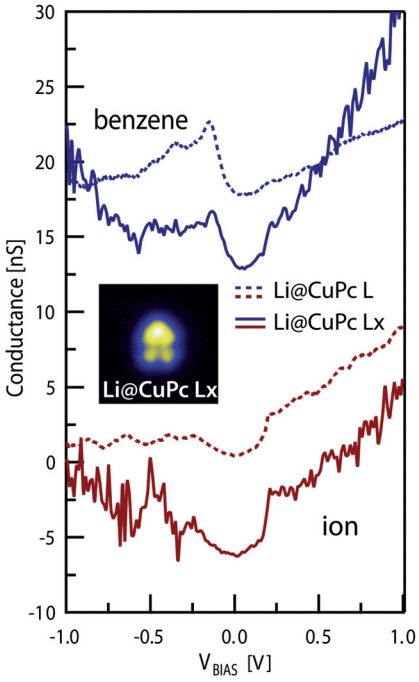

Figure 6.6.: STS of the alternative Li@CuPc L configuration (solid lines) compared to the standard type L complex (dotted lines). (-0.3 V, 0.5 nA). Inset:STM Topography image 5 nm x 5 nm a different geometry for the Li@CuPc Type Lx interaction

We tentatively assign the type L complex to the configuration with the Li adatom underneath the benzene ring, because: (i) the STM images show a clear intense signal coming from one of the benzene rings in these molecules, (ii) no direct topographic indication of a Li adatom on top of the ring is observed, and (iii) the DFT calculations find it to be more stable than the configuration with the Li positioned over the benzene (for NiPc ΔE= 360 meV and for CuPc 390 meV).

Experimentally we observed a different Li@CuPc configuration, which did however occur not very frequently. Figure 6.6 shows a Li@CuPc arrangement, where the Li is situated between two benzene rings, and could be bonded to the aza-N. The STS spectra are identical to those of

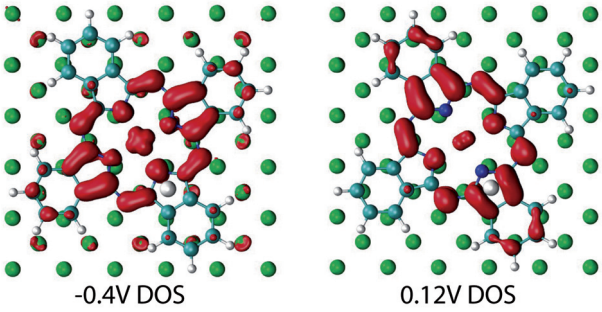

Figure 6.7.: Calculated charge density isosurfaces of the Li@NiPc/Ag(100) system for the occupied α_{2eg} and unoccupied β_{2eg} states. The position of the Li atom is over the benzene ring.

type L configuration, implying a identical electronic structure, matching the results of the DFT calculations.

The calculated PDOS for the Li@MePc complexes is shown in Figure 6.8. Both for CuPc and NiPc the configurations with Li at the benzene show a downshift of the $2e_g$ state further below E_F, confirming the charging of this state due to the Li. The molecule accepts between 1 and 2 electrons, with the exact number slightly varying for each configuration (see Table 6.1), part of the transferred charge originates from the substrate. The electronic structure of the metal ion remains unchanged, with a single electron in b_{1g} ($d_{x^2-y^2}$) in CuPc and none in NiPc.

In general these results are in good agreement with experimental observations. The lifting of the $2e_g$ degeneracy is best seen for Li on top of the benzene ring, where the charge distribution at the lower and upper limits of the $2e_g$ resonance are orthogonal (see Figure 6.4).

The two configurations related to the metal ion reveal a charge transfer channel to the metal ion b_{1g} state. When the Li adatom is slightly shifted from the TM position towards the aza-N, the transferred charge is still located in $2e_g$ in NiPc, but already is accepted by the b_{1g} state in CuPc. This again demonstrates the higher affinity of CuPc to bond via the metal ion d states. We assign the TM-Li configuration to the four-fold symmetric type M, hence here the charge is transferred to b_{1g} state in both molecules. In contrast to the STS results, the uncharging of the $2e_g$ is not reproduced

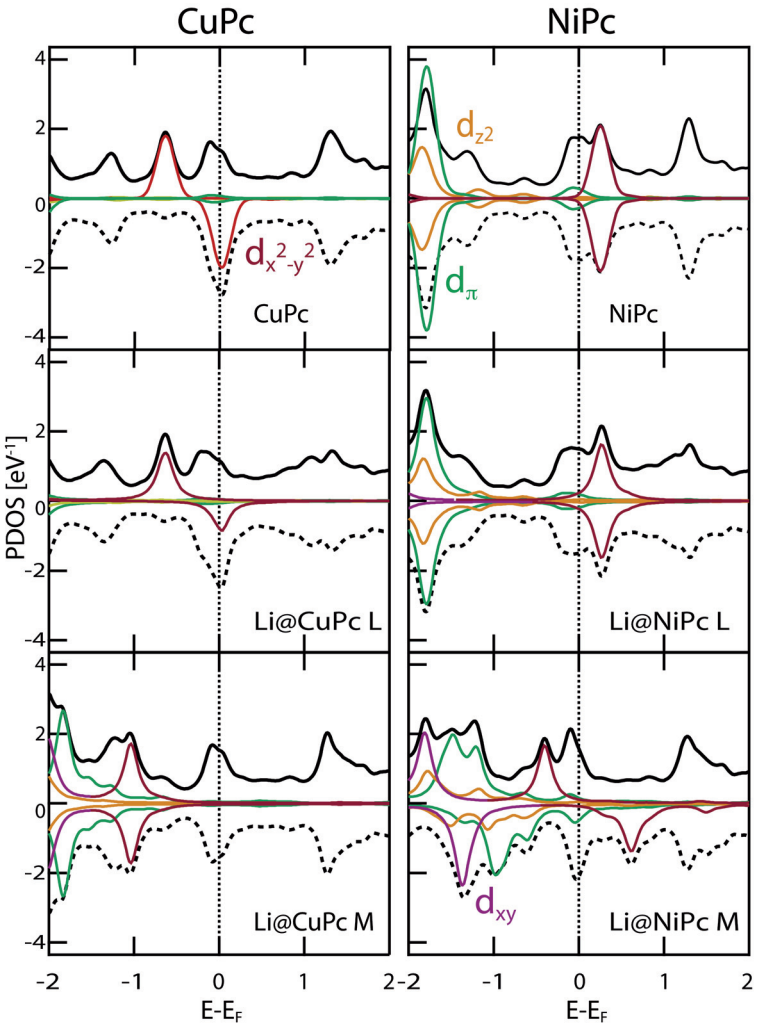

Figure 6.8.: LDA–DFT calculations: spin resolved DOS for NiPc and CuPc molecules with the Li atoms at different sites, corresponding to the benzene (over) and center configurations, projected on the d states of the metal ion.

by the calculations.

In summary, the orbital selective charging of molecules provides a versatile way of creating different charge and spin states in the molecule. For instance, in the case of CuPc, we go from the S=1 state found for the undoped molecule on Ag, to a single spin S=1/2 at the Cu ion in the type L molecule, to an S=0 in the type M.

		aza-N	Under benzene	Over Benzene	Pyrrole	center N3	center
CuPc	ΔE [eV]	0.22	0.49	0.88	0.87	0	0.03
	$m(\mu_B)$	0.44	0.42	0.45	0.42	0	0
	N (total)	1.58	1.44	1.85	1.98	1.98	2.06
	N (Cu)	0.08	0.08	0.09	0.11	0.47	0.66
	N(from Ag)	0.73	0.63	0.98	1.11	1.12	1.1
NiPc	ΔE [eV]	0	0.31	0.67	0.71	0.53	0.99
	$m(\mu_B)$	0	0	0	0	0	0.79
	N (total)	1.38	1.27	1.69	1.8	1.9	2.02
	N (Ni)	0.04	0.04	0.05	0.07	0.15	0.3
	N(from Ag)	0.49	0.47	0.83	0.96	1.02	1.13

Table 6.1.: DFT calculations, for 5 different positions of the Li atom. The energy position is given with respect to the most stable configuration. N denotes the amount of charge transferred to the molecule.

The calculations do not fully reproduce the offset in the charging behavior of CuPc and NiPc, however the general tendency of the latter to accept less charge can be seen in Table 6.1. The charge transfer form the Ag substrate seems to be suppressed by the presence of Li. For MePc/Ag(100) roughly 1 electrons was transferred (Table 5.1 on page 99), whereas for Li@MePc L complexes it is less than 1. The total transfer is generally less than 2 electrons in both molecules. However this value is always smaller for Li@NiPc, closer to 1 than to 2. The interorbital Coulomb repulsion, underestimated by DFT, could stabilize the single charging in Li@NiPc.

The different charging behavior is also seen in gas-phase electron affinity calculations, $[CuPc]^{1-}$ (Electron Affinity* (EA) 0.27eV) accepts an additional electron, more easily than $[NiPc]^{1-}$ (EA 0.8eV) [177]. Using a more

*Positive values mean an additional energy cost.

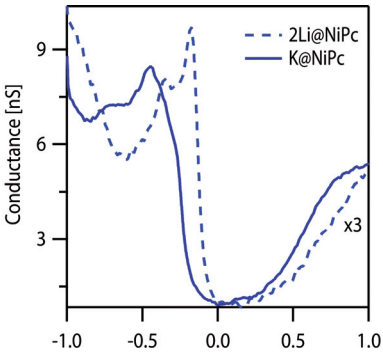

Figure 6.9.: dI/dV spectra taken on one of the benzene rings of L2i@NiPc and K@NiPc (-1 V, 1 nA). The spectra have been shifted for clarity.

electropositive alkali such as Potassium (K), the barrier to doubly occupy the α_{2eg} state can be overcome already with one dopant atom. The STS taken on the K@NiPc L complex is very similar to that of the Li@CuPc L (see Figure 6.9). These arguments confirm that the potential to add a second charge to NiPc is higher than for CuPc.

6.1.1.1. Atom-by-atom doping of CuPc

By using the manipulation capabilities of an STM to move Li atoms onto CuPc molecules, we have created xLi@CuPc complexes with up to 5 Li atoms. Figure 6.10b shows the resulting topographies. The first two Li atoms are localized on opposite benzene rings in the type L configuration. With the introduction of the third Li, however, it becomes difficult to determine the position of all subsequent ones.

In STS taken on the benzene rings, we observe the filling of the α_{2eg} orbital upon the doping with the first Li atom. After the addition of more Li, no further Fermi level crossing of additional peaks is observed, but rather a continuous downshift of the α_{2eg} orbital. This behavior indicates that the charge transfer to the ligand orbitals is saturated. We attribute this to the splitting of the $2e_g$ orbital, which makes it energetically unfavorable to add more electrons to the ligand. Note that from this experiment we cannot exclude the transfer of one additional electron to the single d-hole in the Cu ion.

Our result stands in clear contrast to the observed charging up to the LUMO+2 of a CuPc monolayer on Au(110) doped with K [229]. A possible explanation for this is the geometrical constriction to two dimensions due

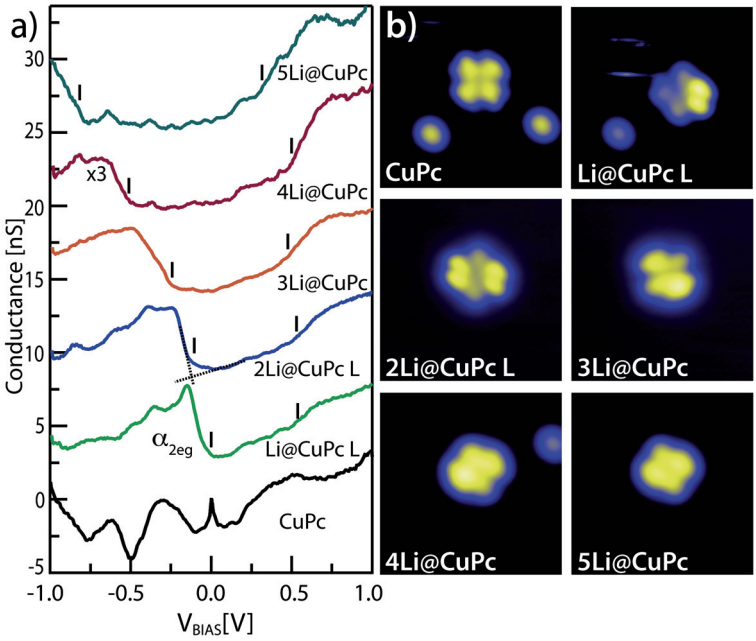

Figure 6.10.: a) dI/dV spectroscopy normalized to conductance units taken on the benzene rings on different xLi@CuPc (-1 V, 1 nA). b) STM topography (-0.3 V, 0.23 nA, 6 nm x6 nm) images showing the addition of up to 5 Li atoms to a single CuPc.

the presence of a metal substrate. Comparable to the case of K doped thin MePc films (100 nm), which show a phase separation for 2K@CuPc and 4K@CuPc phases, with two different geometrical arrangements, where the molecules either accepted two or four electrons from the dopant [227]. However the decreased ionization energy of K compared to Li could also play a role.

Coulomb repulsion:

The addition of Li ions to a Li@CuPc complex after the saturation of charge transfer only affects the gap between α_{2eg} and β_{2eg} orbitals, which increases up to almost a factor of 3. We interpret this as an increased interorbital repulsion, caused by the electrostatic field of the Li ion, based on the linear behavior with the number of Li ions (see Figure 6.11a).

For the Li@NiPc L we find a related effect. Here the proximity of Li ions

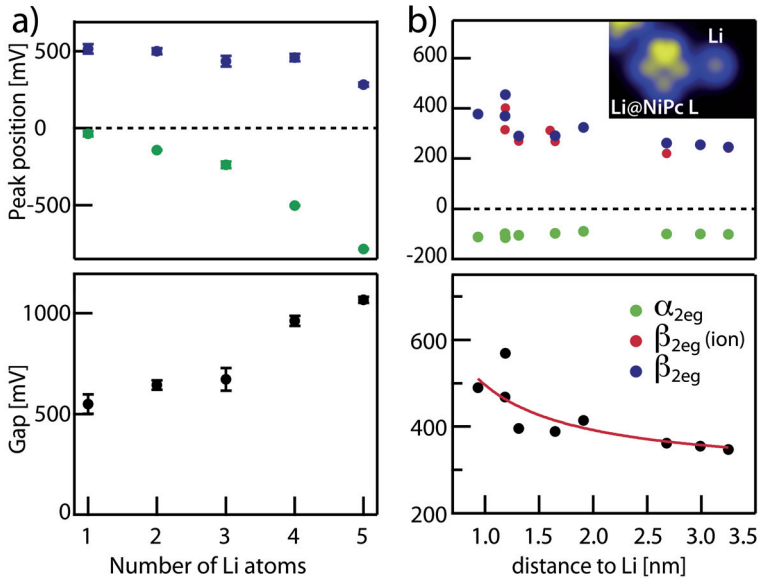

Figure 6.11.: a) Onsets of the STS peaks in Figure 6.10 as a function of added Li atoms for xLi@CuPc (x= 1-5). The resulting gap opens linearly with additional Li atoms. b) Energy position of the α_{2eg}, and α_{2eg}+U orbitals for Li@NiPc in relation to the distance of the nearest Li atom to center of the molecule, blue dots are measured on the benzene, red on the TM center of the molecule (Figure 6.4 shows an example of the STS spectra). The corresponding gap width can be fitted with a 1/r relation. Inset: STM topography of a Li@NiPc with a Li adatom near.

causes the $\alpha_{2eg}+U$ to shift upwards in energy, up to a factor of 2. We study this by measuring the dependence of the intraorbital Coulomb repulsion on the distance between the closest ion and a the center of the Li@NiPc. The distance dependence behavior can be fitted with a 1/r relation (see Figure 6.11b). The increase of the potential as we approach the Li ion can be related to the screening cloud of negative charge surrounding the ion.

In both cases the presence of additional Li affects the energy position of the α_{2eg} orbital, however in the case of CuPc we observe a linear downshift of the fully occupied state, whereas for NiPc the empty $\alpha_{2eg} + U$ state is shifted up. This discrepancy is difficult to explain based on simple electrostatic considerations.

6.1.1.2. Li doping of FePc and CoPc

To further understand the effect of the central ion, also the cases of the paramagnetic molecules FePc and CoPc were investigated. We expect a drastically different behavior due to the ion's out-of-plane d states lying very close to E_F.

The addition of Li gives rise to only one stable configuration each for FePc and CoPc. The stable Li@FePc complex has the same appearance in topography images (see Figure 6.13a) as the FePc/Ag(100) molecule, it can however be distinguished by a height difference (Figure 6.12).

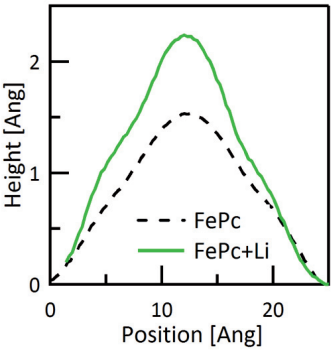

Figure 6.12.: STM Topography height profile for FePc and the Li@FePc complex. (-1V, 0.1 nA)

We conclude that the position of the Li atom is the center of the molecule, similar to the type M configuration found for CuPc. For Li@FePc a deviation from the regualar azimuthal adsorption angle occurs: we observe a $\pm$19° and -37° orientation. The Li@CoPc molecule behaves quite similarly. The stable complex shows an extra protrusion on one of the pyrrole groups, which we interpret as the site of the added Li. The orientation on Ag also becomes unstable and additional angles compared to the regular $\pm$30° are observed (+40°, +14°, -2°, -12°, -22°). This orientation changes might alter the way the molecule interacts with the surface, *i.e.,* the charge transfer from the substrate and the hybridization of the MO.

Nevertheless we observe only a few differences between the undoped and the doped molecules in STS measurements. The spectroscopy on the benzene rings (Figure 6.13c,f) shows a minute downshift of the $2e_g$, which lies still above E_F for both FePc and CoPc. The dI/dV maps taken at the position of these peaks clearly follow the symmetry of the $2e_g$, confirming the origin of these peaks (compare to Figure 5.3 on page 87). On the

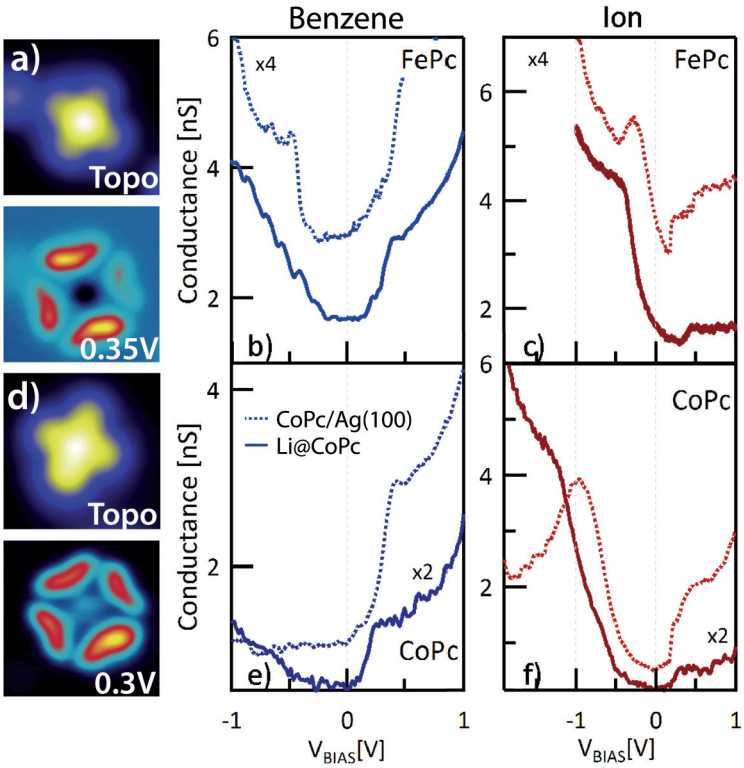

Figure 6.13.: a) STM topography image (-0.5 V, 1vnA) and dI/dV map (0.35 V, 1.1 nA) of FePc showing the uncharged $2e_g$. dI/dV spectroscopy taken on the ion b) benzene c) rings of different the Li@FePc (solid lines) spectra taken on the FePc/Ag(100) are shown as reference (dotted lines) (-1 V, 1 nA). (d,e,f) same for CoPc Topo (-1 V, 0.36 nA) dI/dV map(0.3V, 0.5nA) STS is normalized LiCoPc (-1 V, 0.2 nA) CoPc/Ag(100) (-1 V, 1 nA)

TM, the downshift of the peak corresponding to the $d_\perp$ states is more pronounced (Figure 6.13b), and again very similar for both molecules. For FePc it still crosses Fermi level, which hints towards a situation with not completely filled 3d orbitals. For CoPc the peak is already completely below E_F and shifts from -1V to -1.3V.

The DFT results for the undoped FePc/CoPc in the previous chapter found a complex mixed-valence situation. The molecular orbitals are hybridized with substrate states, and at the same time the ion based e_g

and ligand based $2e_g$ are strongly intermixed. For single Li@FePc and Li@CoPc on Ag(100) it is, thus difficult to quantify the charge transfer, and assign it to specific orbitals without the help of DFT calculations.

6.1.2. Li doping of a monolayer of CuPc

We also studied the effect of Li doping on a complete Monolayer of CuPc molecules adsorbed on Ag(100). The CuPc arrange in a homochiral-dense packed array, with all molecules on each terrace orientated in the same way (see the description in subsection 4.3.2 on page 66). The addition of a small amount of Li atoms, leads to the creation of two different geometrical arrangements (Figure 6.14a,b). Analogue to the M and L structures found for single CuPc, two stable configurations are found. Keeping the same nomenclature, the type M has a bright center, while type L is characterized by two brighter benzene rings compared to the undoped molecules in the layer.

The topographic appearance of type L suggests that the Li atom might be bonded to the aza-N, as two neighboring benzene rings are brighter than the other two. In STS we find a different charging behavior depending on the position of the Li atom analogue to the single molecules complexes. In Figure 6.14c,d the spectra taken on the benzene rings in comparison to those of undoped molecules within the layer are shown. In general the charging behavior is matching that of the single Li@CuPc.

The type M spectra show an unchanged $2e_g$ state above E_F. Following the same argumentation as for the single Li@CuPc M molecule, we reason that the Li transferred one electron to the d states of the Cu ion, reducing its magnetic moment to zero.

For type L complexes the presence of Li induces a splitting of the $2e_g$ again. This can be seen in Figure 6.14d: the charged α_{2eg} state has its intensity only on one of the benzene rings, whereas the unoccupied β_{2eg} is localized on neighboring benzene, revealing an orthogonal symmetry. We can thus conclude that the $2e_g$ state is split and has accepted one electron from the Li atom.

These two configurations are however not equally stable. It is possible by applying a voltage pulse (~ -2.2 V) to irreversibly switch the type M to a type L, as can be seen in Figure 6.14a,b). This indicates that the type M interaction by itself is less stable than type L. On the other hand, as we increase the density of Li atoms this stability criteria is reversed. Figure 6.15c shows the number of type L and M complexes found, as a function of Li

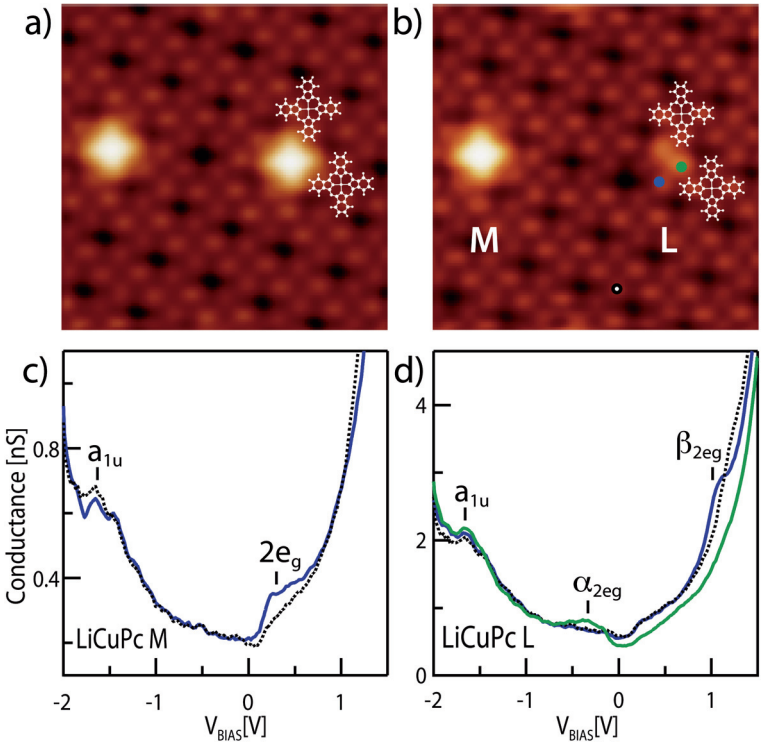

Figure 6.14.: a) STM topography image of two B LiCuPc complexes formed in a monolayer 8.3 nm x8.3 nm (0.2 V, 0.17 nA). b) same region of the sample after applying a voltage pulse on the right M type LiCuPc molecule converting it into the L type c) and d) STS spectroscopy on the Benzene rings of the LiCuPc complexes (-2 V, 0.5 nA with Li and 0.3 nA without Li)

coverage. At low Li dosage both types of configurations can be found on the surface in an approximately equal fraction. With increasing coverage, however, we observe an overall increase of the type M geometry, which eventually becomes dominant over the L type. A possible driving force for this transition could be the electrostatic repulsion between individual Li Ions.

This is in agreement with our XMCD data measured on doped monolayers of CuPc and NiPc, where we can specifically measure the electronic valence and magnetic moment of the metal ion (see Figure 6.16). In both cases we see the transfer of an additional electron to the ion's d states.

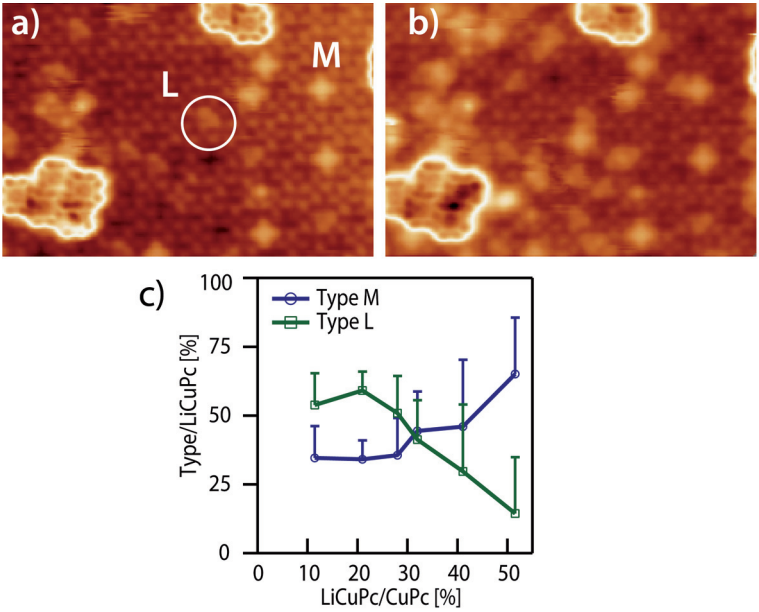

Figure 6.15.: CuPc monolayer a) and b) Topography images for a) low b) and high two Li coverages of the same region (0.2 V, 0.17 nA, 11.5 nm x11.9 nm) c) statistics on the type of interaction as a function of Li coverage, extracted from topography images roughly 500 molecules were counted. Only molecules that were unequivocally identified were used.

The undoped CuPc layer shows a clear magnetic response from the Cu ion, which vanishes upon Li doping. For NiPc layers, we observe the opposite effect, the addition of Li leads to magnetic Ni ion. For NiPc the type M configuration, which was unstable for single molecules seems to be stabilized by the high Li coverage, possibly in the same mechanism causing the crossover of stability in doped CuPc monolayers.

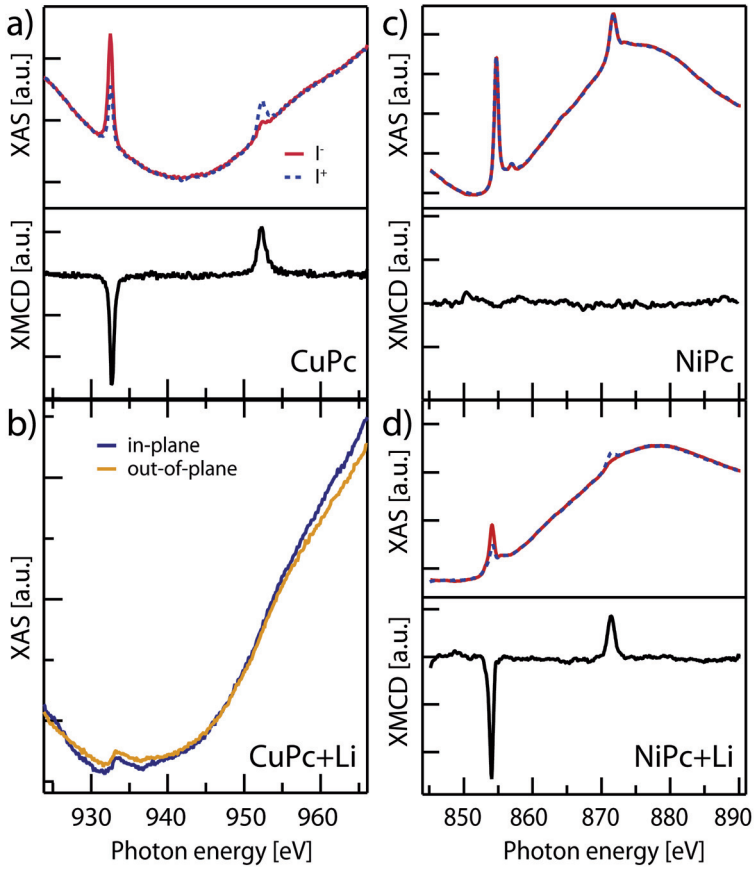

Figure 6.16.: X-ray absorption spectra of CuPc and NiPc monolayer films on Ag(100). a) CuPc film and b) the same film doped with Li, the vanishing signal for the Cu d states indicates the complete filling of the d-shell and a quenching of the magnetic moment for the Cu ion. c) NiPc film, the XMCD measurements shows no magnetic moment for Ni in the undoped film, while d) the NiPc+Li film shows a clear XMCD response for the Ni ion. Measurements taken at T=8 K, normal incidence and 5 T applied field at the ID08 beamline of the ESRF.

6.2. Doping with Fe atoms

The magnetic structure of MePc is strongly influenced by the interaction with the substrate, other molecules and electron donors. The coupling to other magnetic species, could provide another pathway of manipulating the spin structure of these molecules. Using STM and the Kondo effect as a probe, a number of interesting studies on the interaction between magnetic impurities have been published. The antiferromagnetic coupling between an Fe atom and a Kondo screened Co atom on Cu_2N leads to a split Kondo resonance, analogue to the effect an external magnetic field would have [232]. For Co_2 dimers on Au(111), the disappearance of the Kondo resonance has been explained by the reduced exchange coupling between gold conduction electrons and ferromagnetic cobalt dimers [233]. For Ni/Au(111) a decrease in T_K was observed to depend on the distance between two Ni atoms [234]. The broadening of the Kondo resonance was used to determine the strength and sign of of the coupling between two Co atoms on Cu(100) [116]. And finally the coupling between Co atoms through atomic Cu chains was studied: different chain lengths lead to different interactions, where ferro- to antiferromagntic coupling reduced T_K and the RKKY type induced oscillations of T_K [235].

In CuPc the itinerant spin of the organic ligand could act as a coupling between the localized moment of the central ion and the external moment of a magnetic adatom. NiPc, with a similar delocalized moment, but without the magnetic ion, serves to disentangle the effects of the ligand and the ion. We codeposited in two separate preparations CuPc with Fe and NiPc with Fe on a Ag(100) surface, and studied the possible coupling between the magnetic moments of the molecules and the Fe atoms. We observe no evidence of direct magnetic coupling between the Fe and the ligand spin, nor the Cu ion. However, we do observe a change in the Kondo behavior. In case of the Fe atom we see an increase of the Kondo temperature, while for the molecules the Kondo resonance disappears entirely.

Fe atoms on the Ag(100) surface at 5 K show a Kondo interaction with the conduction electrons of the metal (see Figure 6.17d), an effect that has been observed for other magnetic adatoms as well [108, 236, 237]. Fitting a Fano lineshape to the characteristic zero bias peak, and taking the thermal broadening due to sample temperature of 5 K into account (after Ref. [88]) we obtain a Kondo temperature of T_K=37 K (see Figure 6.17e). The uncorrected value of T_K=77 K is close to the uncorrected T_K=80 K

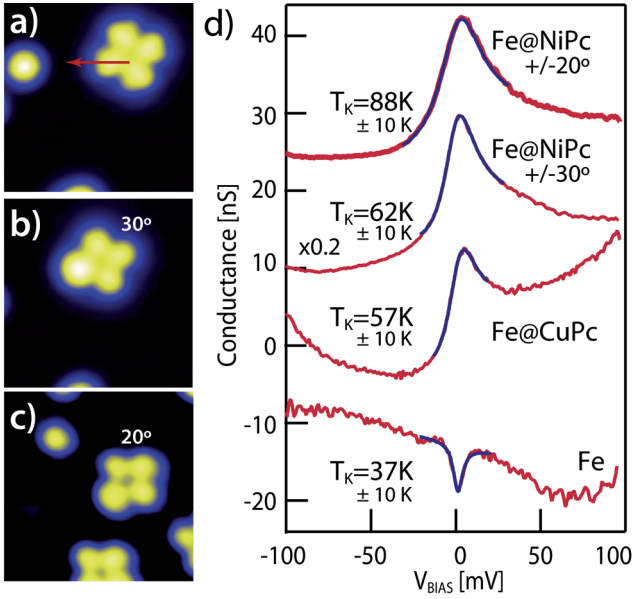

Figure 6.17.: a) Topography of a CuPc and a Fe atom (-0.1 V, 0.1 nA, 5.1 nm x5.1 nm) b) the same region after a lateral manipulation of the CuPc towards the Fe, forming a Fe@CuPc complex. c) Topography of Fe@NiPc with azimuthal orientation of 20° (-0.1 V, 0.1 nA, 5.1 nm x5.1 nm) d) STS and the related Fano fits taken on Fe (-0.1 V, 1.5 nA) and within the Fe@NiPc (-0.1 V, 2 nA) and Fe@CuPc (-0.1 V, 1.5 nA) environments.

found for Fe on Cu100, also measured at 5 K [236].

The in-situ, low temperature deposition of a few Fe atoms on a Ag(100) surface containing single NiPc or CuPc molecules, leads to several interacting configurations between Fe and the molecules. The most common interaction is shown in Figure 6.17b). One Fe atom is directly interacting with one of the benzene rings of the molecule, seen by the brighter appearance in the topography images. Lateral manipulation allows us to verify this composition by pushing a MePc towards a single Fe atom, resulting in the creation of this type B (benzene) interaction (see Figure 6.17a,b,c). The azimuthal orientation of the molecules can change when the Fe is interacting with them. Apart form the known $\pm 30°$, we observe a $\pm 20°$ rotation from the [011] surface axis.

This type of interaction was observed both for NiPc and CuPc equally,

with an identical effect on the spectroscopy. The Kondo resonance and the inelastic vibrational excitations found for the unperturbed molecules disappear completely. The bright lobe, with the Fe atom shows a Kondo resonance (See Figure 6.17d). The corresponding Kondo temperature depends on the azimuthal angle of the molecule, for $\pm 30^{o}$ it has increased to T_K=62 K for Fe@NiPc, and to 57 K for Fe@CuPc, while for $\pm 20^{o}$ Fe@CuPc we find T_K=88 K.

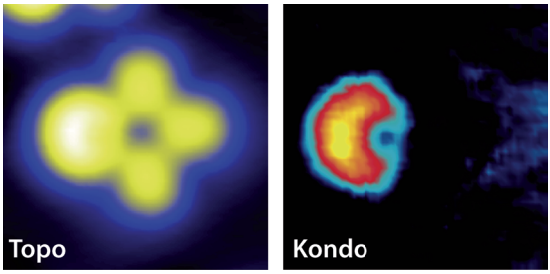

Figure 6.18.: Topography of a Fe@NiPc type B complex (3 mV, 0.2 nA, 2.8 nm x2.8 nm) and the corresponding d^2I/dV^2 map of the Kondo resonance.

The spatial distribution of this Kondo resonance is localized around the benzene ring containing the Fe, facing away from the molecule (see Figure 6.18). This points towards the Fe atom as the origin, while the ligand Kondo of the molecules is quenched. Moreover the type of central ion has no effect, implying that the extra magnetic moment on the Cu^{2+} ion does not couple with the moment of the Fe. We therefore attribute the change in T_K to the interaction with the ligand.

If the Fe is responsible for the Kondo resonance, we observe a change in the Fano line shape, from a dip to a peak. This is associated with different interference conditions between the tunneling into Ag conduction and Fe d states. In this case the contribution of the Ag electrons decreases, a tunneling channel which could be inhibited by the presence of the molecule.

The orientation of the molecule, however, has a noticeable effect, as summarized in Table 6.2. The change in the Kondo temperature of Fe could be related to a change in the local environment, caused by a different adsorption position or the interaction with molecular orbitals. Previous studies have shown that T_K for single adatoms/molecules is extremely sensitive to the local environment, leading to either an increase or a decrease of T_K [111, 113, 237].

	φ	T_K [K] $\pm$10K
Fe close to NiPc	$\pm 30^o$	82
type B Fe@CuPc	$\pm 30^o$	57
type B Fe@NiPc	$\pm 30^o$	62
type B Fe@NiPc	$\pm 20^o$	88
Fe	–	37

Table 6.2.: Summary of the encountered species of Fe@NiPc/CuPc, the azimuthal orientation (φ) of the molecular axis with respect to the [011] direction of the substrate is given, as well as the Kondo temperatures obtained by a Fano function fit of STS data.

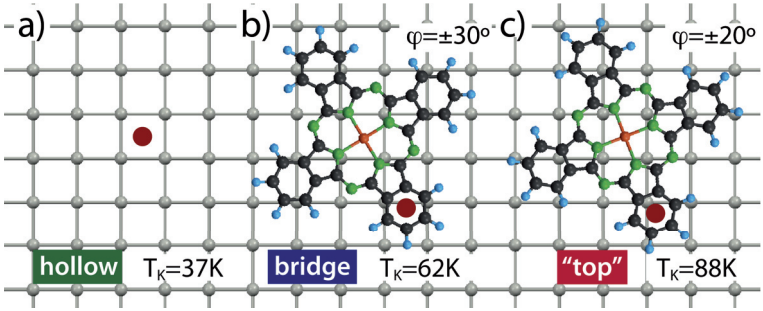

Figure 6.19.: Proposed geometrical model for the type B complexes: The encountered Fe@MePc types and their respective azimuthal orientations have been plotted. The exact position of the Fe is unknown, however if the center of the benzene ring is assumed, the difference in the adsorption sites can be visualized. The center of the molecule is the MePc/Ag(100) hollow site.

If one plots the adsorption geometry of these complexes on Ag(100), a pattern emerges. Depending on the rotation of the molecule, the position of the Fe atoms with respect to the substrate changes (see Figure 6.19). Within this model we can identify three different Kondo temperatures for different adsorption sites of the Fe atom: 57 K for bridge site, 62 K for a "top" adsorption site, and based on observations for Co on Cu(100) [108] the single Fe atom can be assigned to a hollow adsorption site with 37K.

Using lateral manipulation a second Fe atom can be inserted into a MePc molecule. The azimuthal orientation changes during this process and a range of different configurations were observed. All of these

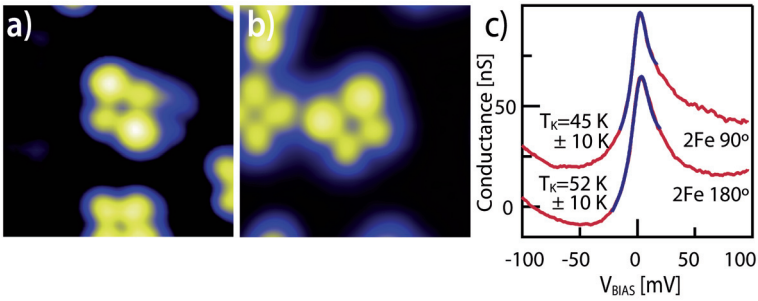

Figure 6.20.: a),b) STM images of two different 2Fe@NiPc configurations (-0.1 V, 0.1 nA, 5.1 nm x5.1 nm) c) The corresponding Kondo resonances, including a Fano function fit.

2Fe@MePc complexes show a Kondo effect at the position of the Fe atoms. The line shape of Kondo resonance is identical to those MePc with a single Fe, equally the T_K lie in the same range from 37 K to 120 K. No dependency of T_K on the number of Fe atoms could be found. Moreover the two complexes shown in Figure 6.20, with the Fe in neighboring or opposing benzene ring have the same Kondo temperature within the error. Based on these facts we conclude that two Fe inside the molecule do not couple. The variations in the Kondo temperature could be a complex variation of the proposed geometric adsorption site effect.

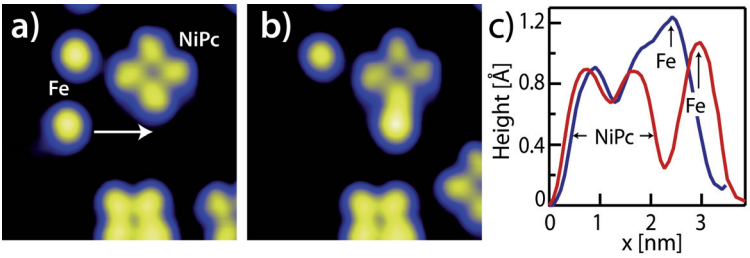

Figure 6.21.: a), b) STM images showing the lateral manipulation to create the interaction between a Fe atom and a NiPc (-0.1 V, 0.1 nA, 5.1 nm x5.1 nm). c) Height profile of a Fe (red) in a) and the Fe close to the NiPc (blue) in b).

We now turn to the other, less common type of interaction observed. A Fe atom that is close enough to a NiPc starts to interact with it. From

topography images, comparing the distance between the center of the Fe and the center of the NiPc, this critical distance can be estimated to be ~2.6 Å. The apparent height of the Fe changes and they appear brighter than the non-interacting ones (see Figure 6.21). Note that it is possible to create the type B interaction by pushing the Fe further towards the molecule (Figure 6.22b).

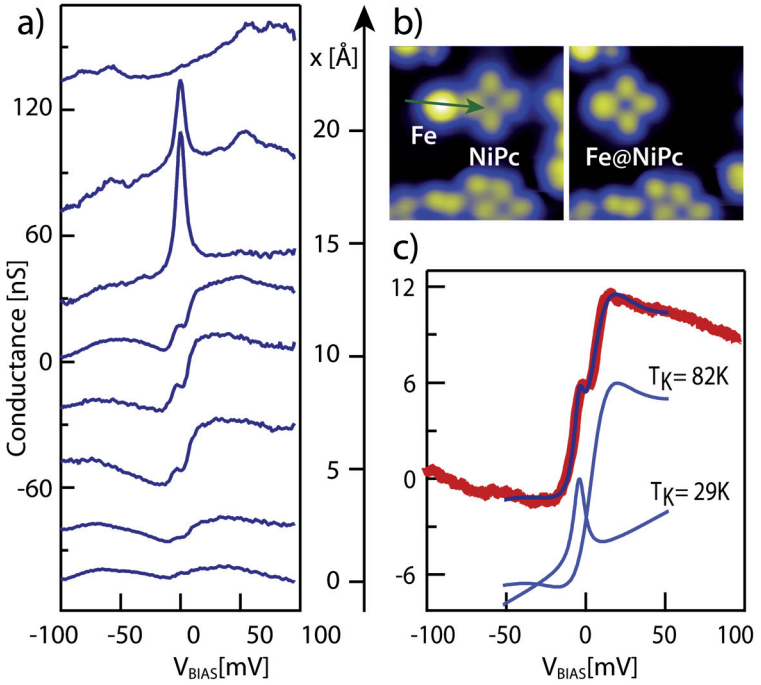

Figure 6.22.: a) various STS spectra (-0.1V, 2nA) taken across a Fe interacting with NiPc, along the green arrow shown in b) the spectra on the botton was taken on the left side of the line. b) Topography images showing an interacting Fe close to NiPc (left), on the right the same molecule is shown after successfully pushing the Fe into molecule converting into a type B (-0.1 V, 0.1 nA, 4.8 nm x4.8 nm) c) Fit of two fano functions for the spectra taken directly on the Fe atom, the T_K=29K was set a parameter, because it is the T_K of the molecule without Fe.

The effect on the spectroscopy is tip position dependent, a series of STS taken along a Fe close to NiPc is shown in Figure 6.22a). Despite the

presence of Fe, the molecule exhibits the typical features for molecules without Fe, i.e., the Kondo resonance with an unchanged T_K=29 K, and the vibrational excitation spectra. On the Fe atom we observe a step like feature, combined with a peak around E_F. Using two overlapping Fano line shapes the feature can be fitted accurately (see Figure 6.22c). For one of the Fano functions, we use the line shape and T_K= 29 K of the unperturbed NiPc/Ag(100). The other Fano function yields a step-like shape with Kondo temperature of T_K =82 K. This value coincides with other T_K found for the type B complexes.

The presence of the unperturbed Kondo resonance of the NiPc points to an overlapping with the one from the Fe adatom when the tip is positioned over the it. The difference in T_K for Fe could be a change in the local environment, like in the case of type B stabilized by the presence of the NiPc. The change in Fano line shape indicates again a decrease of the tunneling to conduction Ag electrons, however not as pronounced as in the case of type B. The greater distance to the molecule could be the reason for this.

6.3. Summary

We have investigated the doping of MePcs (Me= Fe, Co, Ni, Cu) with a charge donor (Li) and spin carrier (Fe) adatoms. For the electron doping we find:

Site-specific charging in CuPc: Depending on the Li-CuPc bonding, charge is transferred to either the ligand or the TM. This mechanism allows to specifically control the spin state (0, $^1/_2$, 1) of the CuPc. For NiPc the two transfer channels are not observed in single molecules because one of them is unstable.

Atom-by-atom charge doping: Multiple doping of CuPc with up to 5 Li, leads to a maximum of 2 electrons transferred, due to the splitting of the degeneracy of the $2e_g$ state, and symmetry constraints imposed by the adsorption.

TM dependence of the total transferred charge: The amount of charge transferred differs for CuPc and NiPc. The lower barrier of CuPc to completely fill the lower part of the split $2e_g$ can be overcome by 1 Li, whereas for NiPc 2 Li or 1 K are required.

Intraorbital and interorbital Coulomb repulsion: The presence of nearby Li ions leads to energy shifts of the α_{2eg} due to intraorbital and

interorbital Coulomb repulsion for Li@CuPc and Li@NiPc respectively.

Electrostatic stabilization of one configuration: With increasing Li coverage for a monolayer of CuPc, the charge transfer observed to the TM's states is preferred, possibly due to electrostatic interaction between the ions.

Magnetic doping with Fe atoms: We have studied the interaction between Fe atoms and NiPc/CuPc molecules on Ag(100). No direct evidence of coupling between the magnetic moment of Fe and MePc was found. Instead the MePc molecules change the local environment of the Fe atoms resulting in changes in the Kondo temperature. A single molecule can embed up to 2 Fe atoms, no evidence of coupling between them was found. The observed T_K was however affected by the azimuthal orientation, probably also related to a change in the Fe adsorption site.

In general we have shown that electron doping is a promising pathway to tune the charge and spin characteristics of for molecules coupled to the substrate via ligand interaction, i.e., CuPc and NiPc. On the other hand for molecules, like FePc and CoPc showing an interaction through the $d_\perp$ orbitals, the results are not conclusive.

The changes in the Fe substrate coupling modulated by the presence of MePcs indicate that these kind of molecules could be used to tune the interaction of magnetic adatoms with metal surfaces.

Chapter 7

7 Conclusions and Outlook

The application of molecules in technological devices depends crucially on the understanding of the behavior on metallic electrodes or substrates. Molecular electronic and magnetic properties, occurring in the gas phase are often times modified or quenched upon adsorption. The results presented in this thesis provide a comprehensive overview of the influence of molecule-substrate and molecule-molecule interactions on the electronic and magnetic structure of molecules adsorbed on a metallic substrate. The mechanisms involved are hybridization of molecular and substrate state, and charge transfer. Our model system were MePc, metal-organic complexes consisting of an organic ligand and a central metal ion, adsorbed on a Ag(100) surface. Investigating four different kinds of MePcs (Me =Fe, Co, Ni, Cu) allowed us disentangle the role of the central ion and the ligand.

The interaction between the MePc and the surface is closely related to the adsorption geometry of individual molecules. In chapter 4 we found that the adsorption of MePc molecules is driven by bond optimization between the ligand with the underlying Ag substrate. Due to this interaction, the flat lying single MePc molecules exhibit two possible orientations of the molecular axis on the surface. The resulting symmetry mismatch between molecule and substrate leads to an asymmetric hybridization of different molecular orbitals. As a result the achiral molecule show chiral contrast in STM topography, without perturbing the chemical structure of the molecules.

As the coverage is increased, intramolecular vdW forces become

important, leading to a transfer of the electronic chirality of single molecules to the organizational level in clusters, independent of the central TM ion. Ostwald ripening of the originally racemic mixture of clusters leads to spontaneous symmetry breaking resulting in mesoscopic homochiral molecular layers. These enantiopure molecular layers and the chirality of distinct molecular orbitals may lead to novel ways to control the electronic properties and optical response of metal surfaces.

In chapter 5 we discussed how the electronic and magnetic properties depend on the whole molecule (ligand and central ion), in contrast to the adsorption geometry, which is determined by ligand-substrate interaction. While all of molecules receive approximately one electron from the surface, depending on type of central ion the, and the character of its frontier d-orbitals, the consequences are different. For d states lying low in energy or within the molecular plane, as is the case for NiPc/CuPc, the main hybridization channels are the organic ligands orbitals, leading to the acceptance of an extra electron here. This unpaired electron causes of an additional magnetic moment in these molecules, whereas the magnetic state of the central ions remains unperturbed. For CuPc intramolecular exchange coupling between d and π electrons leads to the creation a triplet (S=1) ground state.

In contrast to this for FePc and CoPc, with out of plane d-states the interaction through them creates a complex charge reorganization and mixed valence regime. In both cases this interaction leads to a reduction of the ion's magnetic moment.

The influence of molecule-molecule interaction was the second topic in chapter 5. For CuPc molecules we found that the ligand coupling channels with the substrates are strongly affected by neighboring molecules, evidenced by a complex evolution of the electronic structure. In contrast CoPc, interacting mainly through the d states has electronic structure unaffected by intermolecular forces.

The electronic structure and growth of multilayers of CuPc is dominated by molecule-molecule interactions, as the interaction with the substrate becomes screened by underlaying layers. For the electronic structure, we see a trend towards the bulk semiconducting behavior.

In chapter 6 we explored the possibilities of manipulating the electronic and magnetic characteristics of MePc by adding an Li adatoms as electron

donor. Through atom by atom doping of CuPc, we were able to selectively dope ligand and metal states by changing the alkali-molecule bonding configuration. Through this selectivity we were able to achieve a variety of charge (Q) and spin (S) configurations, reaching to Q = 1 and 2 electrons, and S = 0, $1/2$, and 1 with a single alkali dopant. This type of control is a step ahead for the future application of molecules in spintronic devices.

Lastly we have studied the addition of magnetic dopants, in the forms Fe atoms to NiPc and CuPc. We did however observe no direct evidence of a coupling between the magnetic moments of the Fe and the Cu or the ligand. The interaction with molecules however changed the local environment of the Fe atom, and with it, its Kondo temperature.

These findings are important step in understanding the magnetic structure of ligand complexes on surface. The rich magnetic structure of MePc molecules is completely changed by the interaction with a surface. Even though the magnetic moments in MePc are "protected" by the organic ligands, they can be quenched or severely reduced in originally magnetic molecules, and vice versa an additional moment can be induced in diamagnetic ones. The organic component of the molecule, participates in its magnetism leading to fascinating properties such as the intramolecular coupling between ion and ligand spins. Clearly the molecule has to be considered as the whole system ion, ligand, neighboring molecules and surface to understand the full molecular magnetic structure. The detailed step by step investigation (single molecule, cluster, multilayer) allowed us to shed light on the evolution and the mechanism of changes in the electronic structure. The doping with Alkali atoms can be used to control the molecular charge state and magnetic moments. The need for experiments in this area is also underlined, as such effects as the additional ligand spin are difficult to predict from ab-initio calculations.

At several points during the course of this thesis questions were encountered that would make interesting follow up experiments. (i) The electronic structure found for the monolayer of CuPc hinted towards a dispersion of the unoccupied states, possibly due to hybridization with an upshifted surface state. A similar dispersion was observed for TCNQ molecules[203, 204]. The same state showed a strong Stark shift like behavior with the tip sample distance. An investigation of the evolution of this state in function of island size and shape to find the dispersion, might shed light into this problem. (ii) The doping of CoPc and FePc

molecule with Li atoms was not entirely clear, additional DTF calculations might help confirm the charge transfer to the ion, that was found in photoemission studies [222]. (iii) The observed change in Kondo coupling between Fe atoms and Ag substrate mediated by the MePc, suggested that these molecules could be used as templates to shape adatom-substrate interaction [238, 239].

Several pathways of continuing the systematical line of research started in this work present themselves. The role of the substrate can explored in more detail. In this thesis a relative inert noble metal surface Ag(100) was used, but already the interaction with it lead to drastic changes in the molecules. Choosing substrates with either stronger or weaker interaction are a promising next step.

Magnetic surfaces could add an additional interaction dimension. Ferromagnetic samples have already been employed, showing a coupling between the substrate and molecular moments [174, 240, 241, 242, 243]. The ideal complement would be antiferromagnetic surfaces, which could lead to a stabilization of the magnetic moments through exchange bias effects [244, 245]. Relatively easy to prepare in an STM setup would be metal oxide films like NiO, CoO. Studies have shown that flat surfaces can be grown with ease, providing several different layer thicknesses in one preparation [246, 247]. The oxide character might also prove useful as charge transfer to the molecule would be limited. Thin anti-ferromagnetic Mn films on Ag(100) could be a metallic alternative [248, 249].

On the other hand insulating surfaces like NiAl [208] or NaCl [128] have been used to decouple from the electron bath of the substrate metal. These could provide more inert adsorption platform to to study the doping of MePc with Li atoms, with less influence of the substrate like hybridization molecular orbitals, or charge transfer.

Another pathway worth exploring would be amplifying the variety of the chemistry of the organic ligand part. The oxidation state of the central ion can be tuned by using a different ligand or two Phthalocyanine groups, for instance $TbPc_2$ molecules. Further by functionalizing the ligand part of MePc [250], the coupling or bonding to the substrate could be tuned, e.g., sulfonated or thiol-derivatized phthalocyanines would be strongly bonded to the Ag surface through the strong S-Ag affinity. At the same time molecule-molecule interaction can be engineered, polar end groups would lead to stronger hydrogen bond between molecules, creating self-assembled clusters based on them. By carefully choosing these groups a

wide range of network geometries and interaction strengths are possible. These networks, maybe with additional magnetic adatoms, might provide a pathway to create magnetic coupling within a molecular layer.

A Appendix A

CuPcs on Au(111)

To study the influence of the substrate on the charge transfers to the LUMO, we also investigated the adsorption of MePc molecules on different metal surfaces. An obvious choice is another coinage metals like gold. The results show that the type of surface plays a critical role and the maintain exactly the right strength of interaction between the molecule and the surface.

To investigate the influence of the Ag(100) substrate on the charge transfer, we studied CuPc molecules on a Au(111) surface. The preparation was similar to the MePc on Ag(100), on sputter annealed Au(111) surface, CuPc molecules were deposited using the OMBE evaporator (440°C), while the sample was kept at room temperature.

Compared to Ag(100), this surface is less reactive because of the stronger noble-metal character of Au as well as the tighter packed structure of the

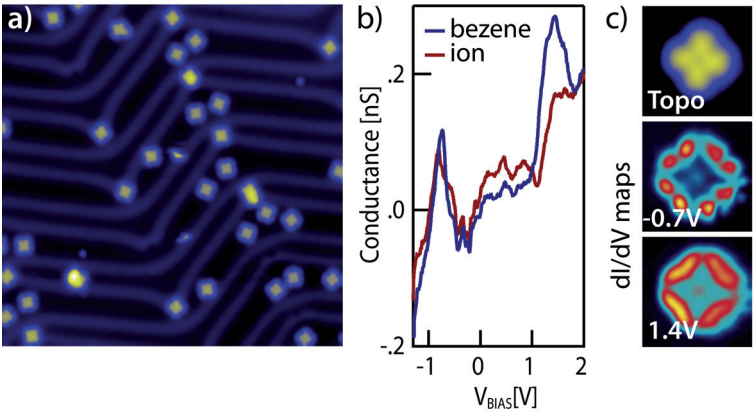

Figure A.1.: a) STM topography image of CuPc molecules on Au(111) surface (-1.2 V 0.1 nA 39 nm x39 nm) b) STS taken on the CuPc on the fcc , blue on the benzene and red on the Cu ion. A spectrum acquired on the bare Au surface has been subtracted to enhance the molecular features (0.25 nA, -1.3V) c) dI/dV maps of the same molecule, showing the a_{1u} state at -0.7 V and the $2e_g$ at 1.4 V 3 nm x3 nm.

(111) plane . This surface presents a more complex reconstruction and several different adsorption site exists [111]. In Figure A.1a) a topography image of the Au(111) surface showing the characteristic herring bone reconstruction is shown. Both possible adsorption sites (fcc, hcp) give the same tendency in STS measurements. Figure A.1b) shows the results for fcc, the a_{1u} and $2e_g$ states can readily be identified, the dI/dV maps taken at these energies (-0.75V and 1.4V) concurs with the $a_{1u}/2e_g$ shapes. The $2e_g$ thus remains unfilled as in the gas-phase, consistent with the fact that no Kondo resonance is observed for this system.